Contribution from the Departments of Chemistry, Oakland University, Rochester, Michigan 48063, and The University of Houston—University Park, Houston, Texas 77004

Electrochemistry and Spectroelectrochemistry of Oxo- and Peroxomolybdenum Porphyrin Complexes

T. Malinski,*[1a] P. M. Hanley,[1a] and K. M. Kadish*[1b]

Received January 16, 1986

The electrochemistry of various oxomolybdenum(IV), -(V), and -(VI) porphyrins is reported in nonaqueous media. The investigated complexes include OMo(TPP), OMo(TPP)(X), O_2Mo(TPP), and $(O_2)_2$Mo(TmTP), where X = ClO_4^-, OCH_3^-, or OH^- and where TPP and TmTP are the dianions of tetraphenylporphyrin and tetra-*m*-tolylporphyrin, respectively. An exact sequence of the individual electron-transfer steps composing the overall redox process of each complex is described, and a comparison between the electrochemistry of the different types of complexes is discussed. Each electrode reaction was monitored by spectroelectrochemistry and by ESR spectroscopy, and on the basis of the electrochemical and spectroscopic data, a self-consistent oxidation–reduction mechanism is presented. The potential for the Mo(V)/Mo(IV) reaction of OMo(TPP)(X) is strongly influenced by the axial ligand X and varies from 0.02 V for X = ClO_4^- to −0.87 V for X = OCH_3^-. OMo(TPP)(X) is produced by the one-electron oxidation and coupled oxygen atom transfer of O_2Mo(TPP) while OMo(TPP) is generated as the final product in the electroreduction of O_2Mo(TPP). This latter reaction involves the addition of two electrons and an ECE mechanism. $(O_2)_2$Mo(TmTP) does not lose the bound peroxo groups upon oxidation or reduction. The single one-electron oxidation of $(O_2)_2$Mo(TmTP) corresponds to formation of a cation radical. In contrast, the first reduction of $(O_2)_2$Mo(TmTP) produces a novel Mo(V) diperoxo complex, which can be further reduced by an additional one-electron-transfer step without loss of the axial peroxo ligand.

A number of papers have described the synthesis, structural and spectroscopic characterization, and chemical reactivity of porphyrins containing Mo(IV), Mo(V) or Mo(VI) as central metal atoms.[2-15] Interest in the chemistry of these synthetic high-valent oxomolybdenum porphyrins has been stimulated by recent studies describing the biomimetic, catalytic, and photochemical behavior of these type complexes.[16-20] Specifically, a clarification of the mechanism of molecular oxygen activation by cytochrome P_{450} dependent monooxygenases is a challenging problem that has aroused considerable interest. Several studies have suggested that high-valent oxoiron metalloporphyrins are involved as the "active oxygen" intermediate.[17,21-23] Thus, the observation of such a reaction in model systems would be of importance for imitating the function of cytochrome P_{450}, as well as providing insights into the electronic and steric effects that affect the reactivity of these oxo complexes.

Recently, one of our laboratories reported preliminary results concerning the electrochemical activation of a metal–oxo bond.[24] This study demonstrated that *cis*-dioxomolybdenum(VI) tetraphenylporphyrin, O_2Mo(TPP), could be oxidized by a one-electron-transfer step followed by an oxygen atom transfer reaction. This is similar to the commonly accepted mechanism for oxidation of cytochrome P_{450} and provides the first example of a simple synthetic high-valent metalloporphyrin exhibiting these characteristics.

A number of other oxomolybdenum porphyrins have also been electrochemically investigated.[8,25-29] For example, the reduction of O_2Mo(TPP)[27] as well as the oxidation and reduction of diperoxomolybdenum(VI) tetra-*m*-tolylporphyrin has been reported in preliminary studies. The reduction of oxomolybdenum(V) tetraphenylporphyrin with a methoxy axial ligand, OMo(TPP)(OCH_3), has also been reported.[29] These results are summarized in the present paper, which describes the overall electrochemistry of different monomeric oxomolybdenum porphyrin complexes containing different trans axial ligands. This paper also describes the electrochemistry of diperoxo and *cis*-dioxomolybdenum(VI) porphyrins. An exact sequence of the individual electron transfer and chemical steps composing the overall redox process is described for each complex, and the interactions between the electrochemistry of the different types of complexes are discussed. These electrochemical studies were carried out in nonaqueous media and include data obtained by voltammetry at a Pt rotating disk electrode, cyclic voltammetry, UV–visible spectroscopy, and ESR spectroscopy.

Experimental Section

Materials. (5,10,15,20-Tetraphenylporphinato)oxomolybdenum(IV), (OMo(TPP)), (5,10,15,20-tetraphenylporphinato)oxomolybdenum(V), (OMo(TPP)(X); X = OCH_3^-, ClO_4^-, and OH^-), *cis*-dioxomolybdenum(VI) tetraphenylporphyrin, and diperoxomolybdenum(VI) tetra-*m*-tolylporphyrin were obtained by methods identical with those reported previously.[2,11,12,20] The supporting electrolytes were obtained from Fisher SG and were recrystallized from absolute ethyl alcohol and then dried in vacuo at 60 °C. Methylene chloride (CH_2Cl_2) and dimethyl sulfoxide (Me_2SO) were obtained from Fisher SG. All solvents were distilled over appropriate drying agents as described in the literature and, in most cases, were stored over 4-Å molecular sieves before use.

Methods. Cyclic voltammetric measurements were made with a PAR Model 173 potentiostat/galvanostat and a Model 178 electrometer probe driven by a PAR 175 universal programmer. An omnigraphic Houston

(1) (a) Oakland University. (b) The University of Houston—University Park.
(2) Ledon, H. *C. R. Seances Acad. Sci., Ser. C* **1978**, *287*, 59.
(3) Ledon, H.; Mentzen, B. *Inorg. Chim. Acta* **1978**, *31*, 139.
(4) Ledon, H.; Bonnet, M. C.; Brigandot, Y.; Yerescon, F. *Inorg. Chem.* **1980**, *19*, 3488.
(5) Srirastara, T. S.; Fleischer, F. B. *J. Am. Chem. Soc.* **1970**, *92*, 5528.
(6) Hayes, R. G.; Scheidt, W. R. *Inorg. Chim. Acta* **1978**, *17*, 1082.
(7) Murakami, Y.; Matsudo, Y.; Yamada, S. *Chem. Lett.* **1977**, 689.
(8) Newton, C. M.; Davis, D. G. *J. Magn. Reson.* **1975**, *20*, 445.
(9) Diebold, T.; Chevrier, B.; Weiss, R. *Inorg. Chem.* **1979**, *18*, 1193.
(10) Ledon, H.; Bonnet, M. C.; Brigandort, Y.; Varescon, F. *Inorg. Chem.* **1980**, *19*, 3488.
(11) Chevrier, B.; Diebold, T. H.; Weiss, R. *Inorg. Chim. Acta* **1976**, *19*, L57.
(12) Matsuda, Y.; Kubuta, F.; Murakami, Y. *Chem. Lett.* **1977**, 1281.
(13) Bains, M. S.; Davis, D. G. *Inorg. Chim. Acta* **1979**, *37*, 53.
(14) Imamura, T.; Takahashi, M.; Tanaka, T.; Jin, T.; Fujimoto, M.; Sawamura, S.; Katayama, M. *Inorg. Chem.* **1984**, *23*, 3752.
(15) Imamura, T.; Tanaka, T.; Fujimoto, M. *Inorg. Chem.* **1985**, *24*, 1038.
(16) Dolphin, D., McKenna, C., Murakami, Y., Tabushi, I., Eds. *Biomimetic Chemistry*; Advances in Chemistry 191; American Chemical Society, Washington, DC, 1980.
(17) Spiro, T. G., Ed. *Metal Ion Activation of Dioxygen*; Wiley-Interscience: New York, 1980.
(18) White, R. E.; Coon, M. T. *Annu. Rev. Biochem.* **1980**, *49*, 315.
(19) Ledon, H.; Bonnet, M. C. *Mol. Catal.* **1980**, *7*, 309.
(20) Ledon, H.; Bonnet, M. C.; Lallemand, T. Y. T. *J. Chem. Soc., Chem. Commun.* **1979**, *704*.
(21) Groves, J. T. Presented at the Symposium on Biomimetic Chemistry—Oxygen Activation, 177 the National Meeting of the American Chemical Society, ACS/CSJ Chemical Congress, Honolulu, HI, 1979; paper ORGN 238.
(22) Fish, R. H.; Kimmel, E. C.; Casider, T. E. *J. Organomet. Chem.* **1976**, *41*, 118.
(23) Ledon, H.; Durbut, P.; Verescon, F. *J. Am. Chem. Soc.* **1981**, *103*, 3601.
(24) Malinski, T.; Ledon, H.; Kadish, K. M. *J. Chem. Soc., Chem. Commun.* **1983**, 1077.
(25) Matsuda, Y.; Yamada, S.; Murokami, Y. *Inorg. Chem.* **1981**, *20*, 2239.
(26) Topich, J.; Berger, N. *Inorg. Chim. Acta* **1982**, *65*, L131.
(27) Ledon, H.; Varescan, F.; Malinski, T.; Kadish, K. M. *Inorg. Chem.* **1984**, *23*, 261.
(28) Kadish, K. M.; Chang, D.; Malinski, T.; Ledon, H. *Inorg. Chem.* **1983**, *22*, 3490.
(29) Kadish, K. M.; Malinski, T.; Ledon, H. *Inorg. Chem.* **1982**, *21*, 2982.

0020-1669/86/1325-3229$01.50/0

Table I. Half-Wave Potentials[a] (V vs. SCE) for 1 mM Oxo- and Peroxomolybdenum Complexes in CH_2Cl_2 Containing 0.1 M TBAP

metal oxidn state	complex	anionic ligand, X	redcn waves						oxidn waves			
			I	II	III	VI	VIII	IX	I	IV	V	VII
Mo(IV)	OMo(TPP)	...		-1.13	-1.48				0.02	1.49		
Mo(V)	OMo(TPP)(X)	ClO_4^-	0.02	-1.13	-1.48					1.48		
		OH^-	-0.10	-1.13	-1.48					1.48		
		OCH_3^-	-0.87	-1.13	-1.48					1.48		
	$[OMo(TPP)(Me_2SO)]^+(X^-)$	OCH_3^-[b]	-0.03	-1.14	-1.49					1.48		
Mo(VI)	$O_2Mo(TPP)$	...		-1.13	-1.48	-0.92				1.49	1.22	
Mo(VI)	$(O_2)_2Mo(TmTP)$	...					-0.09	1.46				1.18

[a] Half-wave potentials were obtained at a rotating disk electrode at a rotation rate of 600 rpm. [b] In Me_2SO containing 0.1 M TBAP.

1000 X-Y recorder was used to record the current–voltage output for sweep rates between 0.02 and 0.30 V/s. Current–voltage curves taken at sweep rates between 0.50 and 50.0 V/s were collected on a Tektronix Model 5111 storage oscilloscope with a camera attachment. Coulometric measurements were performed with a Model 179 digital coulometer. Differential-pulse voltammetric experiments, as well as voltammetry at a rotating platinum-disk electrode, were carried out with an IBM Instruments Model 225 voltammetric analyzer. A conventional three-electrode system was used. This consisted of a platinum working electrode, a platinum-wire counter electrode, and a saturated calomel electrode (SCE) as the reference electrode. All solutions were deoxygenated by passing a stream of purified N_2 into the solution for at least 10 min prior to recording the voltammetric data.

UV–visible spectra were obtained with a Tracor Northern multichannel analyzer. The system was composed of a Tracor Northern 6050 spectrometer containing a crossed Czerny–Turner spectrograph and a Tracor Northern 1710 multichannel analyzer. The spectra result from the signal averaging of 100 5-ms spectral acquisitions. Each acquisition represents a single spectrum from 290 to 917 nm, simultaneously recorded by a double-array detector with a resolution of 1.2 nm/channel. Spectroelectrochemistry was performed in a bulk cell as well as in a thin-layer cell. The bulk cell followed the design of Fajer et al.[30] and had an optical path length of 0.19 cm. The thin-layer cell was a 100 line per inch (lpi) gold minigrid working electrode sandwiched between two glass slides and a platinum-gauze electrode. In both cases, the SCE was separated from the test solution by a fritted bridge containing supporting electrolyte and solvent.

ESR spectra were recorded on a IBM Model ER 100 spectrometer, equipped with an ER 040-X microwave bridge and an ER 080 power supply.

Results

Rotating Disk Voltammetry in CH_2Cl_2. Figure 1 depicts voltammograms of OMo(TPP), OMo(TPP)(ClO_4), $O_2Mo(TPP)$, and $(O_2)_2Mo(TmTP)$, which were obtained at a rotating platinum-disk electrode in CH_2Cl_2 containing 0.1 M TBAP. As seen in Figure 1a, OMo(TPP) undergoes two reductions that occur at -1.13 and -1.48 V (labeled waves II and III) and two oxidations that occur at 0.02 and 1.49 V (labeled waves I and IV). Four processes are also observed for oxidation and reduction of OMo(TPP)(ClO_4) (see Figure 1b). These electrode reactions occur at identical half-wave potentials as for OMo(TPP) (see Table I), and the only difference between the two compounds is that wave I for OMo(TPP)(ClO_4) is a reduction ($Mo^V \rightarrow Mo^{IV}$) while for OMo(TPP), wave I is an oxidation ($Mo^{IV} \rightarrow Mo^V$).

Controlled-potential electrolysis was carried out on the plateau of each wave (150 mV beyond $E_{1/2}$) and indicated that one electron was transferred in each oxidation–reduction step. Limiting currents observed for each of the four oxidation–reduction waves of OMo(TPP) (Figure 1a) and OMo(TPP)(ClO_4) (Figure 1b) were equal in magnitude, and a linear plot of i_l vs. $\omega^{1/2}$ was obtained over a range of rotation rates between 300 and 900 rpm. This fact, as well as the equal currents for each of the four processes, indicates that these four processes each involve the addition or abstraction of a single electron and are mass transport controlled.

The electroreduction of $O_2Mo(TPP)$ proceeds in three steps while the electrooxidation occurs in two steps. The first reduction (wave VI, Figure 1c) is not mass transfer controlled, and a value of $E_{1/2} = -0.92$ V is obtained at a rotation rate of 600 rpm. Waves

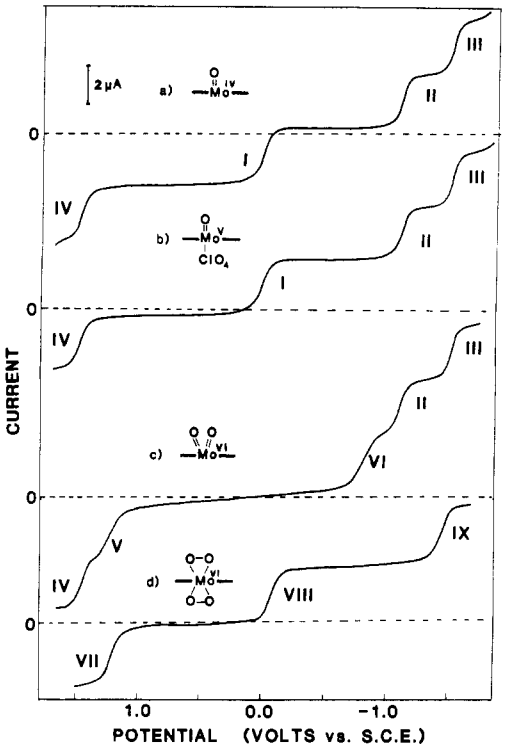

Figure 1. Rotating disk voltammograms illustrating the oxidation and reduction of (a) OMo(TPP), (b) OMo(TPP)(ClO_4), (c) $O_2Mo(TPP)$, and (d) $(O_2)_2Mo(TmTP)$ at a platinum-disk electrode in CH_2Cl_2 containing 0.1 M TBAP. Scan rate = 2 mV/s. Rotation rate = 600 rpm.

II and III occur at -1.13 and -1.48 V and are at potentials identical with those observed for reduction of OMo(TPP) and OMo(TPP)(ClO_4) in this solvent (see Table I). The two electrooxidations of O_2MoTPP are labeled as peaks IV and V in Figure 1c. Stepwise coulometric measurements, first on the plateau of wave V and then on the plateau of wave IV, show that one electron is abstracted in each of the two processes. The first oxidation (wave V, Figure 1c) has a half-wave potential of 1.22 V and plots of i_l vs. $\omega^{1/2}$ indicate that this reaction is controlled by mass transport. The second oxidation (wave IV) occurs at $E_{1/2} = 1.49$ V. This potential is virtually identical with potentials for the oxidation of OMo(TPP) and OMo(TPP)(ClO_4) (see Figure 1 and Table I) and thus suggests a similar reactant for all three complexes.

Only three oxidation–reduction waves are observed for $(O_2)_2Mo(TmTP)$. This is shown in Figure 1d. The waves at -0.09 and -1.46 V are due to reductions, while the wave at 1.18 V is due to oxidation of the complex. All three electrode reactions are mass transport controlled under the applied experimental conditions (300–900 rpm). The shape of the waves suggests the abstraction of one electron in each step, and this was confirmed by controlled-potential coulometry, which yielded a value of 0.98 ± 0.04 faraday in each step.

Cyclic Voltammetry in CH_2Cl_2. Continuous and single-scan cyclic voltammograms were carried out for each of the oxomolybdenum complexes in CH_2Cl_2. Four well-defined reversible redox couples are obtained for OMo(TPP) and OMo(TPP)(ClO_4).

(30) Fajer, J.; Borg, D. C.; Forman, A.; Dolphin, D.; Felton, R. H. *J. Am. Chem. Soc.* **1970**, 92, 3451.

Table II. Absorption Maxima (nm) and Molar Absorptivities ($\epsilon \times 10^{-3}$ M^{-1} cm^{-1}) of Oxo- and Peroxomolybdenum Porphyrin Complexes in CH_2Cl_2

metal oxidn state	complex	anionic ligand, X	λ_{max} ($\epsilon \times 10^{-3}$) Soret band	other bands			ref
Mo(IV)	OMo(TPP)	...	431 (110)		514 (2.0)	554 (10.3)	this work
Mo(V)	OMo(TPP)(X)	Br^-	511 (35.9)		639 (7.4)	685 (8.9)	15
		Cl^-	498 (43)		628 (8.6)	674 (9.3)	10
		NCS^-	496 (45.4)		623 (9.0)	669 (10.1)	15
		ClO_4^-	480 (49)		616 (16)	664 (15)	this work
		OH^-	464 (90)		593 (10.8)	635 (8.4)	10
		$OC_2H_5^-$	457 (128)		583 (14.2)	625 (9.5)	10
		OCH_3^-	454 (170)		540 (3.8)	583 (10.8)	this work
Mo(VI)	O_2Mo(TPP)	...	425 (214)	487 (4.6)	535 (15.2)	562 (11.0)	this work
Mo(VI)	$(O_2)_2$Mo(TmTP)	...	444 (165)	532 (4.0)	572 (25)	613 (30)	this work

The redox couple labeled as peak I in parts a and b of Figure 2 corresponds to the Mo^{IV}/Mo^{V} couple for both complexes.

$$OMo^{IV}(TPP) \rightleftarrows [OMo^{V}(TPP)]^+ + e^- \quad (1)$$

The first reduction of O_2Mo(TPP) (peak VI, Figure 2c) is irreversible in that there is no coupled oxidation peak. At a potential scan rate of 100 mV/s, the cathodic peak potential, E_p, is equal to −0.96 V. The shape of this reduction peak, as well as the scan rate dependence of the peak current, suggests a reaction sequence involving an initial one-electron transfer, which is followed by a chemical reaction and then a further one-electron reduction (an electrochemical ECE mechanism). Reversal of the potential scan, either on the rising portion of peak VI or at potentials more negative than peak VI, yields a new oxidation–reduction couple and E_{pa} = 0.05 V (see Figure 2c). The potential of this oxidation suggests the oxidation shown in eq 1 and, accordingly, this peak is labeled as peak I.

The first oxidation of O_2Mo(TPP) is also irreversible. There is an anodic peak at E_p = 1.25 V (peak V, Figure 2d), which is not coupled to a reverse reduction process. Both the shape of this peak and the current dependence on scan rate suggest a diffusion-controlled one-electron oxidation followed by a fast irreversible chemical reaction (an electrochemical EC mechanism). An additional reversible, diffusion-controlled, one-electron oxidation also occurs at $E_{1/2}$ = 1.49 V (reaction IV). This latter reaction is at a potential characteristic of the OMo(TPP)(ClO_4) oxidation (see Figure 2a,b). Finally, reversal of the potential scan either at 1.4 or at 1.7 V yields a new oxidation–reduction couple, which is characterized by an E_{pc} = −0.01 V. This couple is shown in Figure 2d where the new process is also labeled peak I. Peak I is not observed upon initial reductive scans of O_2Mo(TPP) and, as seen in this figure, is at a potential identical with that for the OMo(TPP)/[OMo(TPP)]$^+$ reaction (eq 1).

A cyclic voltammogram of $(O_2)_2$Mo(TmTP) is shown in Figure 2e and illustrates the presence of three diffusion-controlled oxidation–reduction peaks (processes VII–IX). Diffusion control was verified by the constant values of $i_p/v^{1/2}$ and the invariant values of $E_{1/2}$ with increase in potential scan rate. The potential difference between the anodic and cathodic peak maxima, $|E_{pa} - E_{pc}|$, was equal to 60 ± 5 mV at a scan rate of 100 mV/s, thus indicating the abstraction or addition of one electron in each electron-transfer step. The addition of a single electron at $E_{1/2}$ = −0.09 V was confirmed by controlled-potential coulometry (which gave 1.02 faradays), but coulometric verification of n could not be obtained for the second reduction. Stepping the potential from −0.6 to −1.70 V gave an additional 3 faradays by controlled-potential electrolysis, and the final UV–visible spectrum of the products resembled that of reduced H_2(TPP). This suggests the occurrence of a demetalation reaction that follows the second electroreduction.

Spectroelectrochemical Characterization of Oxidation–Reduction Products in CH_2Cl_2. The molar absorptivities and wavelengths for the major peaks of the four investigated neutral compounds are summarized in Table II. Electronic absorption spectra were monitored before and during the controlled-potential reduction or controlled-potential oxidation of each complex, and typical time-resolved thin-layer spectra are shown in Figures 3–5.

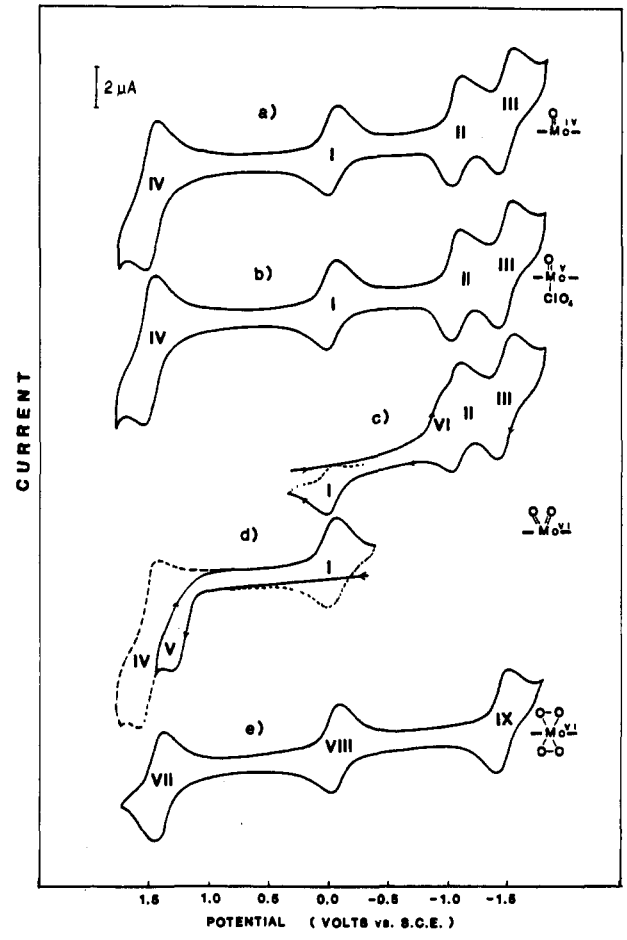

Figure 2. Cyclic voltammograms for the oxidation and reduction of (a) OMo(TPP), (b) OMo(TPP)(ClO_4), (c) O_2Mo(TPP) (initial negative scan), (d) O_2Mo(TPP) (initial positive scan), and (d) $(O_2)_2$Mo(TmTP) in CH_2Cl_2 containing 0.1 M TBAP. Scan rate = 100 mV/s.

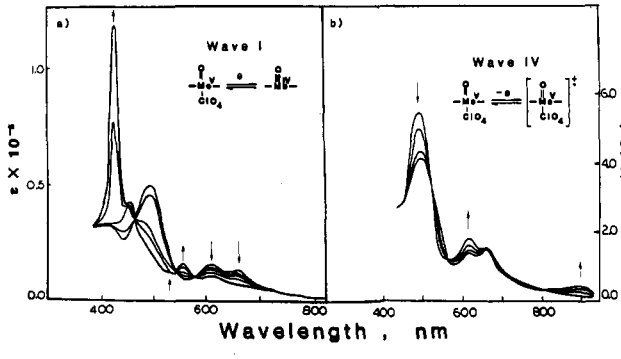

Figure 3. Thin-layer spectra of OMo(TPP)ClO_4 in CH_2Cl_2 containing 0.1 M TBAP during (a) controlled-potential electroreduction at −0.4 V and (b) controlled-potential electrooxidation at 1.48 V.

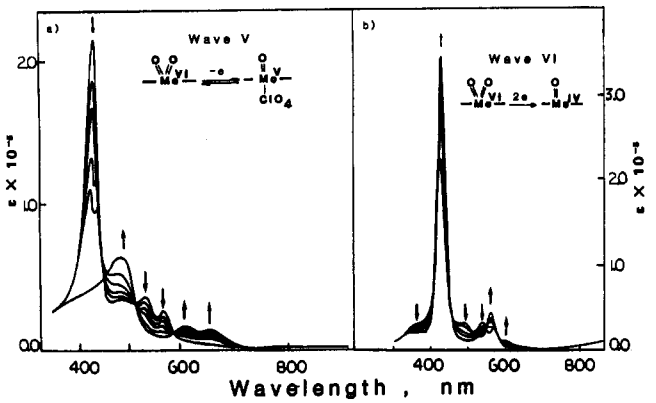

Figure 4. Thin-layer spectra of $O_2Mo(TPP)$ in CH_2Cl_2 containing 0.1 M TBAP during (a) controlled-potential electrooxidation at 1.25 V and (b) controlled-potential electroreduction at −0.96 V.

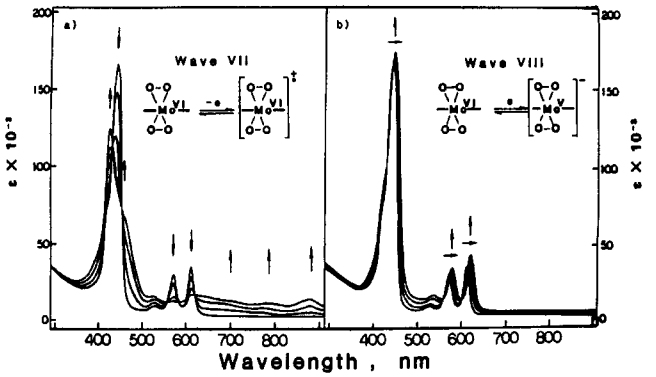

Figure 5. Thin-layer spectra of $O_2Mo(TmTP)$ in CH_2Cl_2 containing 0.1 M TBAP during (a) controlled-potential electrooxidation at 1.5 V and (b) controlled-potential electroreduction at −0.6 V.

Spectra obtained during reduction of $OMo(TPP)(ClO_4)$ at −0.4 V in CH_2Cl_2 are shown in Figure 3a. As the reduction of $OMo(TPP)(ClO_4)$ proceeds, there is a decrease of the Soret peak intensity at 480 nm (which is characteristic of a Mo(V) porphyrin), as well as a reduction of the α and β peak intensity at 664 and 616 nm. At the same time, a new high-intensity Soret band (at 431 nm) and an α and β band (at 514 and 554 nm) appear. These absorbances are characteristic of OMo(TPP). This reduction process is spectrally reversible and switching the applied potential from −0.4 to +0.5 V yields a spectrum characteristic of the $OMo(TPP)(ClO_4)$ starting material. This one-electron-transfer process was found to be reversible by both macro and micro scale electrolysis.

The addition of a second electron to OMo(TPP) produces an unstable species on the time scale of bulk controlled-potential electrolysis. The electronic absorption spectra are characterized by absorbance maxima at 421, 514, 549, 589, and 645 nm after controlled-potential reduction at −1.3 V. These absorbances are identical with those for the singly reduced free base porphyrin anion radical, $[H_2(TPP)]^-$, thus suggesting the overall mechanism:

$$OMo^{IV}(TPP) + e^- \rightarrow [OMo^{IV}(TPP)]^- \quad (2a)$$

$$[OMo^{IV}(TPP)]^- \xrightarrow{\text{demetalation}} H_2TPP + \text{products} \quad (2b)$$

Neutral $H_2(TPP)$ can be reduced by two one-electron-transfer steps, the first of which occurs at $E_{1/2} = -1.25$ V to give the anion radical as shown in eq 3. A second reduction of $H_2(TPP)$ to give

$$H_2(TPP) + e^- \rightarrow [H_2(TPP)]^- \quad (3)$$

$[H_2TPP]^{2-}$ occurs at −1.62 V in CH_2Cl_2. Small reduction peaks in the cyclic voltammograms of OMo(TPP) could be observed at $E_{pc} = -1.28$ and $E_{pc} = -1.62$ V at slow potential scan rates (<50 mV/s) in CH_2Cl_2 and are due to a reduction of free base. These peaks were not observed in cyclic voltammograms of OMo(TPP) that were carried out in more basic solvents such as Me_2SO or pyridine and attempts were thus made to obtain thin-layer UV-visible spectra of $[OMo(TPP)]^-$ or $[OMo(TPP)]^{2-}$ in these solvents. However, the partial demetalation of the first and second molybdenum reduction products were also observed in these solvents, and the obtained spectra were unclear due to the presence of strong bands from $[H_2(TPP)]^-$ or $[H_2(TPP)]^{2-}$.

Spectra obtained during the thin-layer oxidation of $OMo(TPP)(ClO_4)$ (wave IV) are depicted in Figure 3b. As seen in this figure, the Soret peak at 480 nm decreases during oxidation and shifts to 490 nm. At the same time, the β band, which is originally at 616 nm, slightly increases. Also, a new peak which is characteristic for the cation radical[31] appears at about 900 nm.

A spectrum of the product electrogenerated during oxidation of $O_2Mo(TPP)$ is shown in Figure 4a. The final spectrum of the singly oxidized complex is characterized by a Soret peak at 480 nm. This Soret peak and the additional peaks at 616 and 664 nm are identical with those obtained for neutral $OMo(TPP)(ClO_4)$ in the same solvent system (see Table II). The final spectrum of the species obtained during the first controlled-potential reduction of $O_2Mo(TPP)$ (wave VI, Figure 2b) is characterized by a intense Soret peak at 431 nm (Figure 4b). This peak, as well as peaks at 514 and 554 nm, are identical with those reported for OMo(TPP) in CH_2Cl_2.[25] (See Table II.)

Spectra containing Soret peaks at wavelengths greater than 440 nm have been reported for $OMo(TPP)(X)$, where $X = Br^-$, Cl^-, NCS^- and other anions. These spectral data are given in Table II. The final spectrum recorded during the second oxidation of $O_2Mo(TPP)$ (wave IV, Figure 2d) is identical with that presented in Figure 3b and has peaks at 490, 609, 655, and 902 nm. This spectrum is characteristic of a Mo(V) cation radical. However, reversal of the potential from +1.55 to −0.2 V gave a spectrum characteristic of OMo(TPP).

Finally, electronic absorption spectra monitored during controlled-potential oxidation of $(O_2)_2Mo(TmTP)$ (wave VII) are shown in Figure 5a. As seen in this figure, there is a large decrease in molar absorptivity of the Soret band and a shift toward shorter wavelengths on going from $(O_2)_2Mo(TmTP)$ to the product of the first oxidation. The final spectrum has broad absorption peaks from 600 to 900 nm and is characteristic of a cation radical.[31] The formation of this cation radical was spectrally reversible, and the spectrum obtained after controlled-potential rereduction was identical with that of the starting species.

Only small changes in the spectrum of $(O_2)_2Mo(TmTP)$ were observed during the first electroreduction at −0.09 V (wave VIII). This is shown in Figure 5b. Upon the addition of one electron to the Mo(VI) complex, the Soret band shifts by 2 nm toward longer wavelengths while 7- and 9-nm shifts are observed for the α and β bands. This type of shift and the lack of absorbances between 650 and 800 nm strongly suggest a metal-centered reaction. This reduction is reversible on the macroelectrolysis time scale and reoxidation of $[(O_2)_2Mo^V(TmTP)]^-$ gives a spectrum identical with that of the starting species. However, a spectrum characteristic of $H_2(TmTP)$ appears during the second reduction of $(O_2)_2Mo(TmTP)$ (wave IX). This indicates that the product of the second reduction, presumably $[(O_2)_2Mo^{IV}(TmTP)]^{2-}$, is unstable and undergoes a chemical transformation. This second reduction is irreversible on the macroelectrolysis timescale.

Electrochemistry of OMo(TPP)(X) in CH_2Cl_2, Where X = OCH_3^-, ClO_4^-, or OH^-. Cyclic voltammograms of OMo(TPP)(X) complexes, where $X = ClO_4^-$ and OCH_3^-, in CH_2Cl_2 are shown in Figure 6, and half-wave potentials and peak potentials for oxidation and reduction of the investigated complexes are listed in Table I. The electrochemistry of $OMo(TPP)(ClO_4)$ is uncomplicated and has been described above. In contrast, the electrochemistry of $OMo(TPP)(OCH_3)$ is more complicated. Three redox processes are observed for $OMo(TPP)(OCH_3)$ in the range of potentials between +0.10 and −1.7 V. The first reduction occurs at $E_{1/2} = -0.87$ V by rotating disk voltammetry (wave I) and corresponds to a one-electron irreversible reduction of the

(31) Felton, R. H. *The Porphyrins*; Dolphin, D., Ed.; Academic: New York, 1978; Vol. 5, p 53.

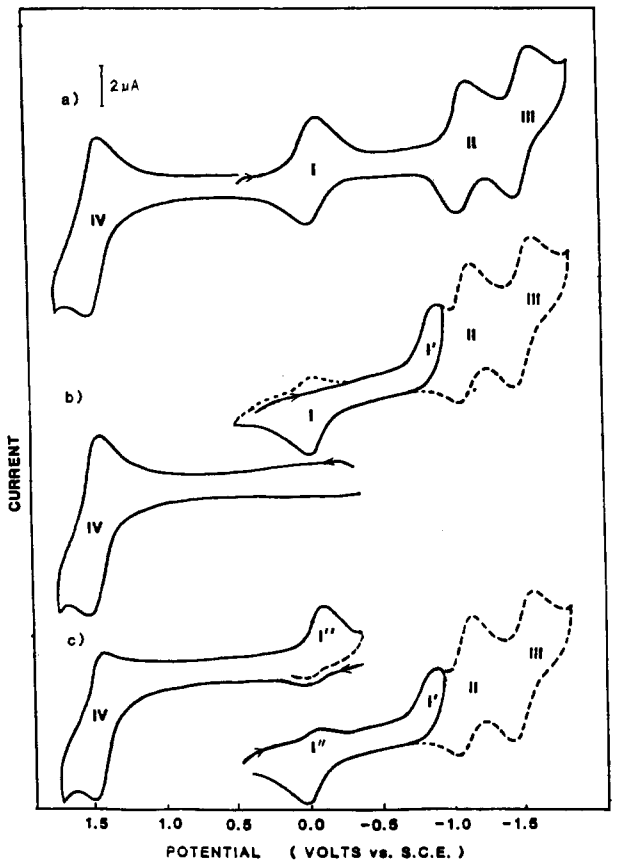

Figure 6. Cyclic voltammograms of (a) $OMo(TPP)(ClO_4)$ in CH_2Cl_2 containing 0.1 M TBAP, (b) $OMo(TPP)(OCH_3)$ in CH_2Cl_2 containing 0.1 M TBAP, and (c) $OMo(TPP)(OCH_3)$ in Me_2SO containing 0.1 M TBAP.

starting complex. Detailed descriptions of this reduction have been presented in a previous paper.[29]

A cyclic voltammogram of $OMo(TPP)(OCH_3)$ is shown in Figure 6b. Process I′ in this figure is irreversible, and the Mo^V complex containing covalently bound OCH_3^- is reduced to the negatively charged Mo^{IV} complex, which still contains bound OCH_3^-. This is shown by eq 4. The singly reduced product is

$$OMo(TPP)(OCH_3) + e^- \rightarrow [OMo(TPP)(OCH_3)]^- \quad (4)$$

not stable at long electrolysis time scales but undergoes dissociation of OCH_3^- to give $OMo^{IV}(TPP)$ and OCH_3^-. Therefore, a reversal of the scan at potentials more negative of peak I′ does not give an anodic peak near −0.8 V but rather gives an anodic peak at ≈−0.05 V (wave I, Figure 6b), which is associated with the reaction shown in eq 5. In a noncoordinating solvent containing TBAP,

$$OMo(TPP) \rightleftarrows [OMo(TPP)]^+ + e^- \quad (5)$$

this ligand associated to Mo(V) will most likely be ClO_4^-. This anion is in large excess compared to OCH_3^-, which is present at $\approx 10^{-3}$ M concentration.

A small reverse reduction peak may be coupled to the oxidation peak at −0.01 V, but this will depend upon the scan rate. In a range of scan rates between 0.5 and 10 V/s the current for the cathodic peak (peak I, Figure 6b) was 70–98% of that observed for the anodic peak. However, at scan rates <0.1 V/s, there was only a small cathodic peak at −0.01 V and the value of i_{pc}/i_{pa} was about 0.2.

Peaks II and III for the reduction of $OMo(TPP)(OCH_3)$ are at the same potential as peaks II and III for the reduction of $OMo(TPP)(ClO_4)$ (Figure 6a) and OMo(TPP). These processes have been ascribed to formation of the Mo(IV) anion radical and dianion respectively.

Cyclic voltammograms obtained for OMo(TPP)(OH) in CH_2Cl_2 are virtually identical with those obtained for $OMo(TPP)(ClO_4)$ in the same solvent system. Both compounds undergo only one oxidation at 1.48 V and two ring reductions at −1.13 and −1.48 V. These same potentials are also observed for the oxidation and reduction of the OCH_3^- complexes in CH_2Cl_2. However, a small difference of half-wave potential is observed for the Mo^{IV}/Mo^V reaction given by wave I. This is shown in Table I, which lists a value of $E_{1/2}$ = 0.02 V for reduction of $OMo(TPP)(ClO_4)$ and −0.10 V for reduction of OMo(TPP)(OH).

Scheme I

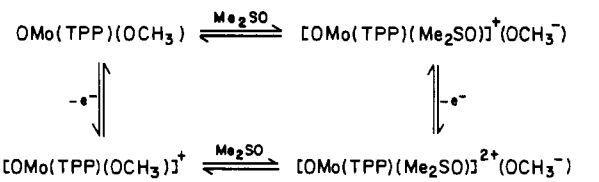

Electrochemistry of $OMo(TPP)(OCH_3)$ in Me_2SO. Four reduction peaks are observed for $OMo(TPP)(OCH_3)$ in Me_2SO. This is shown in Figure 6c. The first reduction (labeled peak I″) occurs at E_{pc} = −0.06 V and is shifted negatively by 50 mV with respect to the first reduction of $OMo(TPP)(ClO_4)$ in this solvent system. This process is most likely due to a reduction of $[OMo(TPP)(Me_2SO)]^+$ to give OMo(TPP). The other three peaks for $OMo(TPP)(OCH_3)$ (labeled peaks I′, II, and III in Figure 6c) occur at potentials about 10 mV more negative than those for the analogous peaks I′ II, and III in CH_2Cl_2 (see Table I). However, the peak current for peak I′ is about 30% lower in Me_2SO (at a scan rate of 0.1 V/s) than that observed for reduction of the same complex in CH_2Cl_2.

The sum of the cathodic peak currents for processes I′ and I″ in Me_2SO are approximately equal to the total peak current for process I′ in CH_2Cl_2. Controlled-potential reduction of $OMo(TPP)(OCH_3)$ at −0.3 V in Me_2SO showed that 0.96 faraday of electrons was transferred during the first reduction. Further stepping of the potential to −0.9 V gave no current. Thus, the cyclic voltammetric and coulometric data indicate that waves I″ and I′ are due to reduction of different Mo(V) complexes that are in equilibrium. One possibility is the equilibrium shown by equation 6. This reaction has been investigated by Imamura et

$$OMo(TPP)(OCH_3) + Me_2SO \overset{K_1}{\rightleftharpoons} [OMo(TPP)(Me_2SO)]^+(OCH_3^-) \quad (6)$$

al.[15] for complexes of OMo(TPP)(X) in CH_2Cl_2/Me_2SO mixtures, where X = Br^-, Cl^-, NCS^-, and F^-. A similar reaction should also occur for X = OCH_3^-.

For potential scans that start at −0.5 V and vary from −0.5 to +1.0 V, the anodic and cathodic peaks I″ are equal in height. However, the cathodic peak I″ is much higher than the anodic peak I″ when the positive potential scan is reversed on the plateau of wave IV (E > +1.5 V) and then scanned in a negative direction. This indicates that the methoxy group bound to the cation radical, $[OMo(TPP)(OCH_3)]^+$, is much easier to replace by Me_2SO than the methoxy group bound to the original $OMo(TPP)(OCH_3)$ neutral complex. This suggests the mechanism given by Scheme I. The presence of a dissociated $[OMo(TPP)(Me_2SO)]^+(OCH_3^-)$ complex is strongly suggested by data from electronic absorption spectroscopy.[15] However, the potentials for oxidation of $OMo(TPP)(OCH_3)$ and $[OMo(TPP)(Me_2SO)]^+(OCH_3^-)$ are very close, and two independent values cannot be determined in the voltammetric measurements.

ESR Spectra of Oxo- and Peroxomolybdenum Complexes in CH_2Cl_2. ESR spectra for Mo(V) porphyrin complexes with different axial ligands have been described in detail.[8,25] The paramagnetic $OMo(TPP)(X)$ complexes exhibit spectra that consist of a strong central line (this occurs at g = 1.9630 for $OMo(TPP)(ClO_4)$ in CH_2Cl_2) and six weak lines symmetrically distributed about the central portion of the spectrum.

The first reduction of $OMo(TPP)(ClO_4)$ (wave I) in CH_2Cl_2 results in a loss of the Mo(V) ESR signal and is consistent with the one-electron reduction of Mo(V) to generate Mo(IV). The second reduction of this complex produces an anion radical ESR spectrum with a g value of 2.0023 at 77 K. This signal is lost

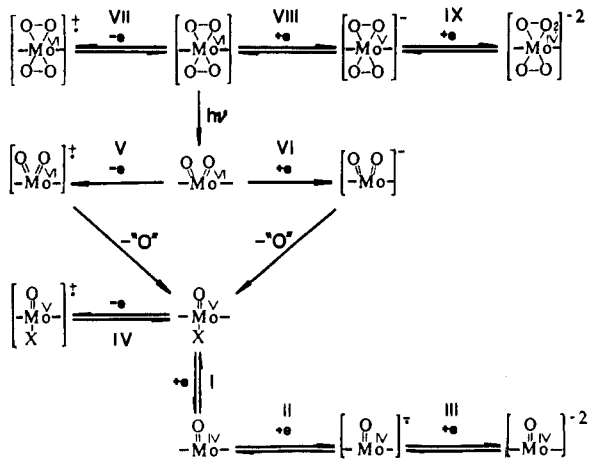

Figure 7. Reaction pathway for the electrochemical oxidation and reduction of oxo- and peroxomolybdenum porphyrin complexes.

after the third reduction. All of these spectra are consistent with the mechanisms presented from the voltammetric data.

The first reduction of $O_2Mo(TPP)$ (wave VI) gives an ESR inactive species, thus suggesting that the product of this reaction is a Mo(IV) complex. In contrast, the first oxidation of $O_2Mo(TPP)$ (wave V) gives an ESR signal which is identical with that observed for $OMo(TPP)(ClO_4)$ in CH_2Cl_2.

Before electrolysis of $(O_2)_2Mo(TmTP)$ no ESR signal is observed. However, after electrooxidation at 1.5 V (wave VII) the radical ESR signal is obtained ($g = 2.0021$). In contrast, controlled-potential reduction at −0.6 V (wave VIII) produces the Mo(V) ESR signal. The spectrum at 295 K has one intense line at the center and six weaker symmetrical bands. The intense absorption is attributed to the ^{96}Mo species, and the $g = 1.9800$ value closely approximates that for the other complexes of OMo(TPP)X.

Discussion

An overall oxidation–reduction scheme for the investigated Mo(VI), Mo(V), and Mo(IV) complexes is shown in Figure 7. This self-consistent scheme is postulated on the basis of the observed electrochemical and spectroscopic data. The electrochemistry of $(O_2)_2Mo(P)$ is well-defined, but this compound may decompose to give $O_2Mo(P)$. Both oxidation and reduction of the *cis*-dioxomolybdenum(VI) porphyrin result in loss of an oxo group, which generates the same OMo(P)(X) species. This species is stable upon oxidation of $O_2Mo(P)$, but upon reduction the potential is such that an overall two-electron transfer occurs and OMo(P) is thus the final product of the electrode reaction.

The simplest electrochemical behavior is observed for OMo(TPP). Only two reductions and two oxidations are observed, both of which consume 1 faraday of electrons in each step. The product of the first electroreduction (wave II) is assigned as due to formation of an anion radical, which can be reduced further to give the dianion (wave III).

$$[OMo(TPP)]^{\cdot-} + e^- \rightarrow [OMo(TPP)]^{2-} \quad (7)$$

Unfortunately, the second reduction products could not be characterized by either UV–visible or ESR spectroscopy. This was due to a demetalation reaction that followed formation of the anion radical on the macroscale electrolysis time scale. However, it is quite clear that OMo(TPP) undergoes two reversible one-electron reductions at −1.13 and −1.48 V before decomposition occurs. These values of $E_{1/2}$ are shifted positively by 120 mV relative to those for reduction of $H_2(TPP)$.

The absolute potential difference between the first and second reduction potentials of OMo(TPP) is 0.35 V and this agrees with the 0.35–0.40-V range for the formation of anion radicals and dianions of other metalloporphyrins.[32] Also, the difference between the first ligand oxidation and the first ligand reduction of OMo(TPP) is 2.64 V. This is comparable to that reported for OMo(OEP)(OH),[32] but is larger than that obtained for other metalloporphyrins.

The one-electron reduction of OMo(TPP)(X) to give OMo(TPP) is easily monitored by UV–visible and ESR spectroscopy, and the generated oxomolybdenum(IV) complex was stable under anaerobic conditions for at least 10 days.

The *cis*-dioxomolybdenum porphyrin complex is reduced by a sequence of steps involving an overall two-electron transfer. These electron-transfer processes sandwich a homogeneous chemical reaction. In this ECE mechanism (eq 8–10), a protonation (arising

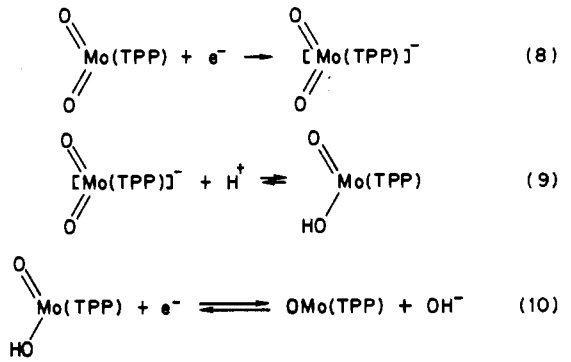

either from the solvent or from minor traces of water) follows after the first electron-transfer step and yields OMo(TPP)(OH), which has a reduction potential of $E_{1/2} = -0.10$ V. (See Table I.) Therefore, a second one-electron-transfer reaction can take place at the potential of reaction 8 (which is about 750 mV more negative than the reduction potential of OMo(TPP)(OH)), producing an apparent overall two-electron reduction. A similar mechanism, as shown in eq 8–10, was also observed at 223 K, but attempts to spectrally identify the site of the first reduction (i.e., metal center, oxygen atom, or π-ring system) were unsuccessful due to the rapid protonation step (eq 9), which produced OMo(TPP)(OH). Studies of the diperoxomolybdenum(VI) complex (see the following discussion) show that an initial one-electron reduction (wave 8) occurs at the metal center, yielding a Mo(V) species. However, this possibility can be neither ascertained nor ruled out for the *cis*-dioxomolybdenum(VI) complex.

An electron may be abstracted from the central metal, from the conjugated porphyrin ring system, or occasionally from a bound axial ligand of a metalloporphyrin.[33] For the $O_2Mo(TPP)$ complex, abstraction of an electron from Mo^{VI} or from the oxo ligand is not possible and the only reasonable site of oxidation is from the π-ring system, thus producing the cation radical $[(O_2)Mo(TPP)]^{\cdot+}$. However, the UV spectrum of this species could not be obtained within the lower time scale of thin-layer spectroelectrochemistry (~0.1 s). Also, no ESR spectrum was observed at 293 or 77 K. In fact, the only observed ESR spectrum (and UV–visible spectrum) was that of $OMo(TPP)(ClO_4)$, which is produced by loss of an oxo ligand from $[O_2Mo(TPP)]^{\cdot+}$.

Since isosbestic points are observed at $\lambda = 445$, 518, and 590 nm during electrooxidation of $O_2Mo(TPP)$ (Figure 4a), one can only assume that very low concentrations of the radical are present in solution and that the chemical reaction (oxygen atom transfer) is faster than the time scale of the electrochemical and spectroelectrochemical measurements. This would imply that this radical is highly reactive, unlike $O_2Mo(TPP)$, which is only a mild oxidizing agent.

The initial steps in the electrochemical oxidation of $O_2Mo(TPP)$ (eq 11) are similar to the commonly accepted mechanism for oxidation of cytochrome P_{450} (eq 12). The oxidation product of

$$O_2Mo^{VI}(P) \xrightarrow{-e^-} [O_2Mo^{VI}(P)]^{\cdot+} \xrightarrow{-O} [OMo^{V}(P)]^{+} \quad (11)$$

$$[OFe^{IV}(P)]^{\cdot+} \xrightarrow[-SO]{+S} [Fe^{III}(P)]^{+} \quad (12)$$

(32) Fuhrhop, J.-H.; Kadish, K. M.; Davis, D. G. *J. Am. Chem. Soc.* **1973**, *95*, 5140.

(33) Kadish, K. M. *Prog. Inorg. Chem.* **1986**, *34*, 435–605.

the Mo(VI) porphyrin loses an oxo function and contains a central metal in a lower oxidation state than the parent compound. This is similar to the case of cytochrome P_{450}. However, for the case of molybdenum an additional oxidation is observed. The second electrooxidation product is assigned as a cation radical. This radical is $[OMo(TPP)(X)]^{\bullet+}$ which is generated from OMo(TPP)(X) as shown in Figure 7 (wave IV).

The first oxidation of $(O_2)_2Mo(TmTP)$ (wave VII) leads to a cation radical that is stable on the controlled-potential electrolysis time scale. This is demonstrated by the fact that controlled-potential rereduction of $[(O_2)_2Mo(TmTP)]^{\bullet+}$ generates the original spectrum. The cation radical was found to be stable up to 15 h. Symmetrical peroxo groups probably stabilize this radical. This is in contrast to $O_2Mo(TPP)$, which has cis oxo groups but forms a very unstable cation radical after electrooxidation.

The electroreduction of $(O_2)_2Mo(TmTP)$ produced a Mo(V) diperoxo porphyrin complex that is also stable, and the original spectrum could be obtained upon controlled-potential reoxidation. The reduction product of the second one-electron addition to $(O_2)_2Mo(TmTP)$ is formally assigned as a diperoxomolybdenum(IV) complex. However, attempts to spectrally identify the site of the second reduction (i.e., metal or porphyrin ring based) were unsuccessful due to decomposition of $[(O_2)_2Mo(TmTP)]^{2-}$ at longer than cyclic voltammetry time scales of electrolysis. In all cases, only $[H_2(TmTP)]^{2-}$ and some form of a Mo(IV) porphyrin complex were obtained. Evidence for the latter molybdenum oxidation state in the decomposition product comes from cyclic voltammetry after bulk electrolysis. Under these conditions a wave was observed at potentials characteristic of the Mo(IV)/Mo(V) porphyrin couple.

The interesting and significant aspect of the above mechanism is that reduction of $(O_2)_2Mo(TmTP)$ appears to be at the central metal and not at the porphyrin ring. Almost all known tetraphenylporphyrin derivatives show ring reductions that occur between −1.0 and −1.8 V vs. SCE, and the majority have potential separations of 300–470 mV between $E_{1/2}$ values for formation of the anion radical and dianion.[33] This is not the case for $(O_2)_2Mo(TmTP)$. Thus, the alternate explanation of π-radical formation after reduction of $(O_2)_2Mo(TmTP)$ can be ruled out on the basis of the reduction potential for wave VIII, the large potential separation between wave VIII and wave IX, and the nonradical electronic absorption spectrum illustrated in Figure 5b. Of special importance is the fact that electrogeneration of a stable $[(O_2)_2Mo(TmTP)]^-$ complex provides the first example where a peroxo-bound metalloporphyrin can be reduced at the central metal without affecting the nature of the metal–oxygen bond.

It has already been noted that ligands bound trans to the oxo group of a Mo(V) tetraphenylporphyrin complex are labile, and equilibrium constants for reactions of $OMo(TPP)(OCH_3)$ with Cl^-, OAc^-, and ClO_4^- ligands in CH_2Cl_2 have been reported as 0.1, 6.3×10^{-3}, and 4.3×10^{-5}, respectively.[25] The substitution reactions of OMo(TPP)(X) by Me_2SO in CH_2Cl_2 have also been studied by UV–visible spectroscopy.[15] The spectrum changes in two steps as the concentration of Me_2SO in CH_2Cl_2 is increased from 0 to 20% (v/v). The hypochromic shift is 1–2 nm in the first stage of the reaction and has been ascribed to a solvation of the complex by Me_2SO. The second stage involves significant changes of the Soret band absorbance and has been described as due to a substitution reaction between the anionic ligand, X, of OMo(TPP)(X) and Me_2SO. Formation constants for this reaction were determined as 180, 0.88, and 0.80 for X = Br^-, Cl^-, and NCS^- ligands, respectively. These types of substitution reactions were also observed in our electrochemical studies, and for the case of the $OMo(TPP)(OCH_3)$ complex this led to a number of different reduction waves.

Finally, it should be noted that all of the OMo(TPP)(X) complexes lose the anionic ligand after formation of Mo(IV). This does not appear to be the case for OMo(TPP)NCS, where NCS^- remains bound even after generation of the anion radical and dianion.[26] In this case, complexation by NCS^- results in a small positive shift of potential for waves II and III. These processes have been reported as occurring at −0.988 and −1.363 V in Me_2SO containing 0.05 M TBAP. These values can be compared to potentials of −1.14 and −1.49 V for reduction of $OMo(TPP)(OCH_3)$ in the same solvent system.

Acknowledgment. The support of the National Science Foundation (K.M.K.; Grant 8215507) and Oakland University (T.M.; research fellowship) is gratefully acknowledged.

Registry No. TBAP, 1923-70-2; OMo(TPP), 33519-60-7; $[OMo(TPP)]^-$, 74751-82-9; $[OMo(TPP)]^{2-}$, 74751-83-0; $[OMo(TPP)]^+$, 88437-51-8; $[OMo(TPP)]^{2+}$, 102978-43-8; $OMo(TPP)(ClO_4)$, 77321-00-7; $[OMo(TPP)(ClO_4)]^-$, 102978-44-9; $[OMo(TPP)(ClO_4)]^{2-}$, 103067-93-2; $[OMo(TPP)(ClO_4)]^{3-}$, 102978-45-0; $[OMo(TPP)(ClO_4)]^+$, 102978-46-1; OMo(TPP)(OH), 28780-74-7; $[OMo(TPP)(OH)]^-$, 102978-47-2; $[OMo(TPP)(OH)]^{2-}$, 102978-48-3; $[OMo(TPP)(OH)]^{3-}$, 102978-49-4; $[OMo(TPP)(OH)]^+$, 102978-50-7; $OMo(TPP)(OCH_3)$, 74751-79-4; $[OMo(TPP)(OCH_3)]^-$, 68220-78-0; $[OMo(TPP)(OCH_3)]^{2-}$, 102978-51-8; $[OMo(TPP)(OCH_3)]^{3-}$, 102978-52-9; $[OMo(TPP)(OCH_3)]^+$, 102978-53-0; $[OMo(TPP)(Me_2SO)]^+(OCH_3^-)$, 102978-42-7; $[OMo(TPP)(Me_2SO)](OCH_3^-)$, 102978-55-2; $[OMo(TPP)(Me_2SO)]^-(OCH_3^-)$, 102978-57-4; $[OMo(TPP)(Me_2SO)]^{2-}(OCH_3^-)$, 102978-59-6; $[OMo(TPP)(Me_2SO)]^{2+}(OCH_3^-)$, 102978-61-0; $O_2Mo(TPP)$, 78229-89-7; $[O_2Mo(TPP)]^-$, 102978-62-1; $[O_2Mo(TPP)]^{2-}$, 102978-63-2; $[O_2Mo(TPP)]^{3-}$, 102978-64-3; $[O_2Mo(TPP)]^+$, 102978-65-4; $[O_2Mo(TPP)]^{2+}$, 102978-66-5; $(O_2)_2Mo(TmTP)$, 87371-95-7; $[(O_2)_2Mo(TmTP)]^-$, 87371-97-9; $[(O_2)_2Mo(TmTP)]^{2-}$, 102978-67-6; $[(O_2)_2Mo(TmTP)]^+$, 87371-96-8.